Growth and properties of epitaxial GdN

B. M. Ludbrook,[1,a)] I. L. Farrell,[2] M. Kuebel,[1] B. J. Ruck,[1] A. R. H. Preston,[1] H. J. Trodahl,[1] L. Ranno,[3] R. J. Reeves,[2] and S. M. Durbin[2]
[1]*The MacDiarmid Institute for Advanced Materials and Nanotechnology, School of Chemical and Physical Sciences, Victoria University, P.O. Box 600, Wellington 6140, New Zealand*
[2]*The MacDiarmid Institute for Advanced Materials and Nanotechnology, University of Canterbury, Private Bag 4800, Christchurch 8140, New Zealand*
[3]*Institut Néel, CNRS/UJF, BP 166, 38042 Grenoble Cedex 9, France*

(Received 18 May 2009; accepted 20 July 2009; published online 23 September 2009)

Epitaxial gadolinium nitride films with well-oriented crystallites of up to 30 nm have been grown on yttria-stabilized ziconia substrates using a plasma-assisted pulsed laser deposition technique. We observe that the epitaxial GdN growth proceeds on top of a gadolinium oxide buffer layer that forms via reaction between deposited Gd and mobile oxygen from the substrate. Hall effect measurements show the films are electron doped to degeneracy, with carrier concentrations of 4×10^{20} cm^{-3}. Magnetic measurements establish a T_C of 70 K with a coercive field that can be tuned from 200 Oe to as low as 10 Oe. © *2009 American Institute of Physics*. [doi:10.1063/1.3211290]

I. INTRODUCTION

The rare-earth nitrides (RENs) have recently gained attention, with significant advances in treating the theoretical problem of their electronic and magnetic properties.[1–5] Those computations have suggested electronic band structures that show strong coupling between the spin and charge degrees of freedom, suggesting the potential for use of these materials in spintronic applications. In particular, in the ferromagnetic ground state, there is a strong exchange splitting of both the valence and conduction bands of order 0.5 eV,[3,4] so that both electrons and holes share the same spin polarization. Similar exchange splitting has been exploited to demonstrate highly polarized spin injection across a ferromagnetic EuO tunnel barrier.[6]

However, the experimental situation is still far from clear, owing to the instability of these materials in air, along with the difficulty of growing well-ordered materials with stoichiometric RE:N ratios and low levels of oxygen.[7–9] GdN is the most thoroughly studied of the REN compounds; Gd has a half filled 4*f* shell with zero orbital angular momentum and a large spin moment of $7\mu_B$ in the common Gd^{3+} ionization state. GdN is well established as ferromagnetic below a Curie temperature (T_C) of 70 K.[10–14] Recent measurements of stoichiometric polycrystalline films show it to be a narrow-gap semiconductor both above and below T_C.[10,15]

Recent developments have begun to point the way toward the growth of stoichiometric films and effective capping procedures for passivating RE-N films against oxidation. Most of that work has been on nanocrystalline films.[10–12,14] One study has described epitaxial growth of GdN on MgO substrates, but no details of the resulting electronic or magnetic properties are available.[16] In this paper, we describe the heteroepitaxial growth of thin film GdN using a plasma-assisted pulsed laser deposition (PLD) technique and discuss the electrical and magnetic properties of the layers.

a)Electronic mail: bartludbrook@gmail.com.

II. SAMPLE GROWTH AND CHARACTERIZATION

GdN thin films were grown on double-side polished (100)-oriented yttria-stabilized zirconia (YSZ) substrates that were degreased by 5 min immersion in each of trichloroethylene, acetone, and methanol before transfer to the growth chamber (base pressure 10^{-9} Torr). Substrates were outgassed at 800 °C for a minimum of 1 h. A Lambda Physik Compex 205 KrF excimer laser with wavelength of 248 nm and pulse length of 25 ns was operated at a repetition rate of 10 Hz with an energy density at the target ranging from 2 to 8 J cm^{-2}. A 99.9% purity elemental Gd sputtering target was employed for GdN growth and a YSZ substrate was used as a target for film capping. 99.999% pure nitrogen gas was passed through an Aeronex filter to an Oxford Applied Research HD25 rf plasma source operated at powers ranging from 120 to 400 W and pressures ranging from 2.5×10^{-5} to 1.2×10^{-4} Torr. Target-to-substrate distance was fixed at 6.0 cm. Growth was monitored *in situ* using a 20 kV Staib reflection high energy electron diffraction (RHEED) system in conjunction with a KSA 400 CCD imaging system. Magnetic susceptibility measurements were made on a quantum design MPMS superconducting quantum interference device. Hall effect and magnetoresistance measurements were performed in the four terminal Van der Pauw geometry, with chromium and gold dual layer contacts deposited directly onto the capping layer.

Samples of thickness ranging from 60 to 180 nm, as determined by Rutherford backscattering spectrometry (RBS), were grown at temperatures from room temperature up to 850 °C and capped with 30 nm of YSZ. For temperatures above 700 °C epitaxial growth is observed, as demonstrated by the [100] RHEED images from a sample grown at 800 °C shown in Fig. 1. The initial substrate pattern [Fig. 1(a)] shows streaks with a spacing corresponding to the YSZ lattice constant of 0.512 nm, as well as Kikuchi lines demonstrating the high crystalline quality of the substrate. As the growth of GdN progresses [Fig. 1(b)], the streaks become bold and elongated, indicating high quality, epitaxial crystal

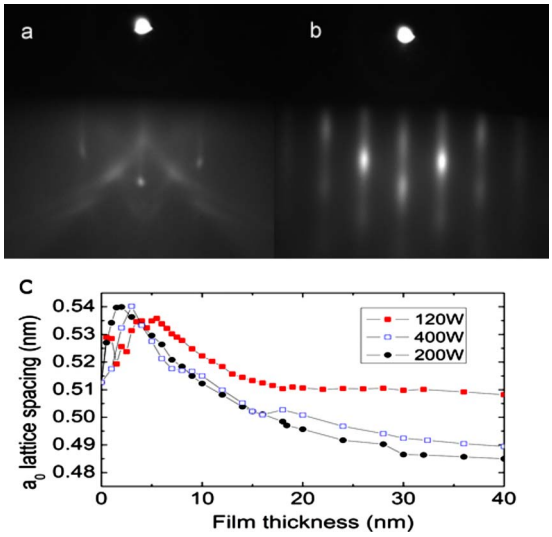

FIG. 1. (Color online) RHEED images taken along the [100] direction from (a) the substrate, and (b) the GdN film after 60 min growth at 800 °C. The GdN layer takes the same orientation as the substrate and the streaky lines are indicative of long range crystalographic ordering on the surface. (c) The in-plane surface lattice spacing can be extracted from the RHEED data and is plotted as a function of film thickness for three films grown with different nitrogen plasma power.

growth, although a small amount of surface roughness is apparent in the slightly spotty nature of the RHEED patterns. Taking RHEED along the [110] substrate direction, we extract a near surface lattice spacing a factor of $\sqrt{2}$ larger than that along [100], as expected for cube on cube epitaxy.

Epitaxial films showed no systematic variation in quality across the temperature range 700–850 °C. Nitrogen plasma power was varied from 0 to 400 W; the full width at half maximum (FWHM) of the central RHEED streak at 200 W was found to be 50% smaller than for the other power values after 30 min of growth. Samples grown at lower temperature ($T<700$ °C) were polycrystalline and nonepitaxial, although x-ray diffraction (XRD) indicates these films are strongly textured in the [001] direction. We have reported previously that GdN can be grown in inert nitrogen.[10] This remains true, but we can now add that the crystal quality is improved for samples grown in activated nitrogen with a moderate plasma power.

Figure 2 shows a typical XRD pattern from GdN confirming the strongly epitaxial character of the films grown on

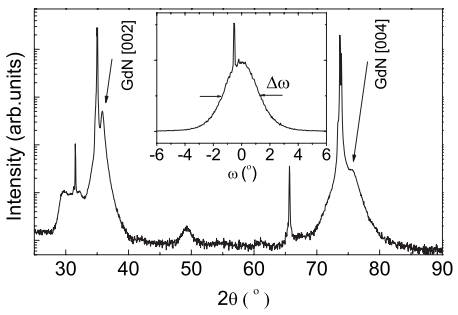

FIG. 2. 2θ XRD showing only the GdN [00n] peaks. The single crystal substrate [00n] peaks are seen adjacent to the GdN lines at lower angle. Inset: A rocking curve with a FWHM of 2.4° indicates the layers have significant mosaic spread.

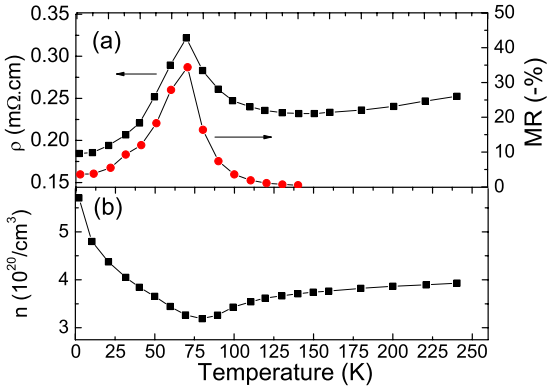

FIG. 3. (Color online) (a) Temperature dependent resistivity (black squares, left axis) and magnetoresistance (red circles, right axis) both show a peak at T_C. (b) Carrier concentration, n, as a function of temperature determined from Hall effect measurements. Transport anomalies at T_C in (a) correlate with changes in the carrier concentration in (b).

[001] oriented YSZ. Only the [002] and [004] peaks appear with significant intensity, and we extract an average lattice constant of 0.500 ± 0.002 nm. The lines are narrow, with FWHM values as low as 0.3° in the best samples from which we obtain an approximate bulk coherence length of 30 nm using the Scherrer formula. This quantity will be referred to below as the crystallite size, although for these films it is likely to be dominated by lattice dislocations rather than distinct crystallites. Rocking curves reveal up to 1° of tilt between the substrate and film lattice planes. The 2.4° FWHM of the rocking curve peak (inset, Fig. 2) indicates the presence of mosaic spreads, which implies a high density of dislocations.[17]

Monitoring the in-plane lattice spacing as a function of film thickness in the early stages of growth [Fig. 1(c)], we see a sharp increase from the substrate lattice spacing to roughly 0.54 nm, consistently peaking at film thicknesses of 2–4 nm suggesting it is an interfacial phenomenon. Cubic gadolinium oxide (Gd_2O_3) has the Gd ions in an fcc arrangement and a lattice constant of 0.541 nm,[18] and given the affinity of gadolinium for oxygen[16] and the mobility of oxygen in YSZ,[19] it is likely that Gd_2O_3 forms at the interface by incorporating oxygen from the substrate. The full role of the Gd_2O_3 layer in the epitaxy is not yet understood, although it almost certainly limits the overall crystalline order. For now, we note that it is an insulator and as such does not affect the transport properties described below. Interstitial incorporation of oxygen into GdN has been shown to make the material difficult to magnetize to saturation.[9] This is not observed in these films, implying there is no significant diffusion of oxygen from the oxide buffer layer into the GdN layer.

III. RESULTS AND DISCUSSION

Figure 3(a) shows the temperature-dependent resistivity from the film shown in Fig. 1, along with the magnetoresistance $[\rho(0T)-\rho(4T)]/\rho(0T)$. In the paramagnetic state ($T>70$ K), both the magnitude of the resistivity and its positive temperature coefficient indicate that the film is a semiconductor doped to degeneracy. The carrier density inferred from the Hall effect [Fig. 3(b)] supports this view. The ob-

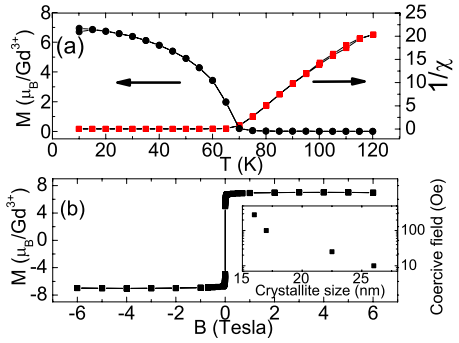

FIG. 4. (Color online) (a) Temperature dependent magnetization (left axis) for a GdN sample grown at 800 °C showing ferromagnetism below 70 K saturating at the expected value of $7\mu_B/\mathrm{Gd}^{3+}$. The inverse susceptibility is plotted on the right axis showing paramagnetic behavior above a T_C of 70 K. (b) Field loops measured in-plane saturate to the expected value in small applied fields. Inset: The coercive fields of various samples at 10 K correlate with the ordered length scales determined by XRD.

served doping is likely due to *N* vacancies, as both we and others have concluded previously.[10,14] The sign of the Hall coefficient indicates that the carriers are electrons. The room temperature carrier density would correspond to no more than 1% vacancy on the *N* sites, below the detection limit by RBS and nuclear reaction analysis. Using values for the resistivity and carrier concentration shown in Fig. 3, and assuming a free electron effective mass $m^*/m=1$, we calculate a room temperature mean free path of 11 nm, comparable to the crystallite radius.

The magnetization measurements shown in Fig. 4(a) from a film deposited at 800 °C exhibit the familiar GdN ferromagnetic response below 70 K.[10,14] Plotting the inverse susceptibility (right axis) shows Curie–Weiss behavior, giving a Curie temperature of close to 70 K. In the ferromagnetic state, the moment is easily saturated at 10 K to $7\mu_B/\mathrm{Gd}$ ion in low fields applied in-plane. Both T_C and the saturation moment are in agreement with data on the best GdN in the literature, but the coercive field is just 10 Oe lower than any previously reported. As shown in the inset of Fig. 4(c), this is closely related to the crystallite size determined by XRD, with the coercive field at 10 K decreasing by more than an order of magnitude as the ordered length scale rises by a factor of 2. The ease with which the direction of magnetization can be switched is an important material characteristic when considering spintronic applications of GdN such as spin valves. The present result demonstrates that in GdN it can be tuned in a controlled manner by adjusting the growth conditions. Determining the exact nature of the magnetic interactions in GdN is an outstanding problem.[5,20,21] It is interesting to note that we see no significant difference in T_C between these heavily doped films and samples reported previously with lower carrier concentrations,[10,14] suggesting that the exchange interaction is not mediated by free carriers.

We observe the anomalous Hall effect (AHE) at temperatures nearing and below T_C, as the magnetization of the sample becomes significant. The AHE contributes a Hall resistance approximately proportional to the magnetization and the high-field slope returns the ordinary Hall coefficient. The implied carrier concentration is plotted in Fig. 3(b). The apparent dip near T_C is slightly uncertain, for the magnetization does not reach full saturation in this temperature range. On the other hand, the data signal a clear 30% increase between ambient temperature and 10 K which correlates well with the lower resistivity of the ferromagnetic state. Such an increase is expected in view of the established narrowing of the GdN band gap in the magnetically ordered state.[14,15]

Negative magnetoresistance (represented here as the fractional resistance change in a field of 4 T) was observed at all temperatures, with a large peak at T_C. These data are plotted in Fig. 3(a) with the resistivity data to illustrate the striking similarity of the temperature dependence. The resistivity around T_C can be reduced by 35% in the presence of a large magnetic field and the anomalous peak at T_C is observed to shift to higher temperatures, as reported also by Luenberger *et al.*[14] However, at low temperatures, the sample is well ordered and the application of a magnetic field has little effect.

IV. CONCLUSION

In summary, we have grown epitaxial GdN by PLD. The spontaneous formation of an oxide buffer layer has been identified and related to the mobility of oxygen in the YSZ substrate. It has been shown that these samples are degenerate semiconductors and the free carriers are electrons. The drop in resistivity below T_C is related to an increase in the carrier concentration as the material becomes ferromagnetic. We find that the coercive field is dependent on the crystallite size, a result that implies the former may be tuned.

The MacDiarmid Institute is supported by the New Zealand Centre of Research Excellence Fund and the research reported here is supported by Grant No. VICX0808 from the New Economy Research Fund.

[1] C. G. Duan, R. F. Sabiryanov, J. Liu, W. N. Mei, P. A. Dowben, and J. R. Hardy, Phys. Rev. Lett. **94**, 237201 (2005).
[2] A. Chantis, M. van Schilfgaarde, and T. Kotani, Phys. Rev. B **76**, 165126 (2007).
[3] C. M. Aerts, P. Strange, M. Horne, W. M. Temmerman, Z. Szotek, and A. Svane, Phys. Rev. B **69**, 045115 (2004).
[4] P. Larson, W. R. L. Lambrecht, A. Chantis, and M. van Schilfgaarde, Phys. Rev. B **75**, 045114 (2007).
[5] C. Mitra and W. R. L. Lambrecht, Phys. Rev. B **78**, 134421 (2008).
[6] T. S. Santos, J. S. Moodera, K. V. Raman, E. Negusse, J. Holroyd, J. Dvorak, M. Liberati, Y. U. Idzerda, and E. Arenholz, Phys. Rev. Lett. **101**, 147201 (2008).
[7] F. Hulliger, *Handbook on the Physics and Chemistry of Rare Earths* (North Holland Physics, New York, 1978), Vol. 4, pp. 153–236.
[8] O. Vogt and K. Mattenberger, *Handbook on the Physics and Chemistry of Rare Earths* (Elsevier, Amsterdam, 1993), Vol. 17, pp. 301–407.
[9] R. J. Gambino, T. R. McGuire, H. A. Alperin, and S. J. Pickart, J. Appl. Phys. **41**, 933 (1970).
[10] S. Granville, B. J. Ruck, F. Budde, A. Koo, D. J. Pringle, F. Kuchler, A. R. H. Preston, D. H. Housden, N. Lund, A. Bittar, G. V. M. Williams, and H. J. Trodahl, Phys. Rev. B **73**, 235335 (2006).
[11] F. Leuenberger, A. Parge, W. Felsch, F. Baudelet, C. Giorgetti, E. Dartyge, and F. Wilhelm, Phys. Rev. B **73**, 214430 (2006).
[12] K. Khazen, H. J. von Bardeleben, J. L. Cantin, A. Bittar, S. Granville, H. J. Trodahl, and B. J. Ruck, Phys. Rev. B **74**, 245330 (2006).
[13] R. A. Cutler and A. W. Lawson, J. Appl. Phys. **46**, 2739 (1975).
[14] F. Leuenberger, A. Parge, W. Felsch, K. Fauth, and M. Hessler, Phys. Rev. B **72**, 014427 (2005).
[15] H. J. Trodahl, A. R. H. Preston, J. Zhong, B. J. Ruck, N. M. Strickland, C. Mitra, and W. R. L. Lambrecht, Phys. Rev. B **76**, 085211 (2007).
[16] L. W. Gerlach, J. Menning, and B. Rauschenbach, Appl. Phys. Lett. **90**,

061919 (2007).
[17]B. Heying, X. H. Wu, S. Keller, Y. Li, D. Kapolnek, B. P. Keller, S. P. DenBaars, and J. S. Speck, Appl. Phys. Lett. **68**, 643 (1996).
[18]R. W. G. Wyckoff, *Crystal Structures* (Interscience, New York, 1964), Vol. 2, pp. 3–5.
[19]M. Weller, R. Herzog, M. Kilo, G. Borchardt, S. Weber, and S. Scherrer, Solid State Ionics **175**, 409 (2004).
[20]C. G. Duan, R. F. Sabiryanov, W. N. Mei, P. A. Dowben, S. S. Jaswal, and E. Y. Tsymbal, Appl. Phys. Lett. **88**, 182505 (2006).
[21]T. Kasuya and D. X. Li, J. Magn. Magn. Mater. **167**, L1 (1997).